

# Dynamic Systems Modelling

Coursework Simulink-based modelling

Candidate #13442

University of Bath - Department of Mechanical Engineering

December 2023

---

**Keywords:** Car Model, Suspension, Wheel, Road, Speed Bump, Simulink

---

## CONTENTS

<b>1. Introduction</b>	<b>3</b>
<b>2. Model Construction and Verification</b>	<b>4</b>
1. Body Model . . . . .	4
2. Suspension Model . . . . .	7
3. Wheel Model . . . . .	8
4. Complete half-car Model . . . . .	10
<b>3. Investigation of Car Performance</b>	<b>15</b>
1. Sinusoidal Road . . . . .	15
2. Speed Bump . . . . .	17
2.a. Car Behaviour . . . . .	17
2.b. Passenger Comfort Optimisation . . . . .	19
<b>A Appendix: Source Code</b>	<b>22</b>
<b>References</b>	<b>26</b>

## LIST OF FIGURES

1	Speed bump integrated with pedestrian crossing (Brancquart, 2017) . . . . .	3
2	Representation of a half-car with two suspensions (Cookson, 2023) . . . . .	4
3	Half-Car body icon block. . . . .	5
4	Free fall test body movement . . . . .	6
5	Force equilibrium test body pitch . . . . .	6
6	Lifting force test body movement . . . . .	7
7	Lifting force test body pitch . . . . .	7
8	Half-Car suspension icon block. . . . .	7
9	Half-Car wheel icon block. . . . .	8
10	Free fall test wheel movement . . . . .	9
11	Force equilibrium test wheel . . . . .	10
12	Road step test wheel movement . . . . .	10
13	Half-Car model assembly. . . . .	11
14	Stationary car test body and wheel movement . . . . .	12
15	Road step test body movement with a rigid wheel . . . . .	12
16	Road step test body and wheel movement with a rigid suspension . . . . .	13
17	Suspension spring non-linear coefficient . . . . .	13
18	Non-linear comparison on a stationary car test showing body and wheel movement . . . . .	14
19	Road step test body movement with non-linear parameters . . . . .	14
20	Sinusoidal road test body movement with amplitude $A = 0.01m$ . . . . .	16
21	Sinusoidal road test body movement with velocity $v = 10ms^{-1}$ . . . . .	17
22	Watts and Seminole profile speed bumps (Shwaly, Zakaria and Al-Ayaat, 2018) . . . . .	17
23	Car movement while driving at $8m/s$ over a single Watts profile speed bump around 5.5s . . . . .	18
24	Car movement while driving at $8m/s$ over a single Seminole profile speed bump around 4.3s . . . . .	19
25	Human body vertical acceleration exposure limits according to ISO (2018) . . . . .	20
26	Optimisation boundary around the speed bump induced acceleration . . . . .	20
27	Comparison between the non-optimised and optimised suspensions on the car body movement . . . . .	21
28	Simulink body subsystem . . . . .	22
29	Simulink suspension subsystem . . . . .	23
30	Simulink wheel subsystem . . . . .	23
31	Simulink tests for each subsystem of the car model . . . . .	23
32	Simulink tests for the car model . . . . .	24
33	Simulink tests for sinusoidal road effect . . . . .	24
34	Simulink setup for a Watts profile speed bump . . . . .	24
35	Simulink setup for a Seminole profile speed bump . . . . .	25
36	Simulink tests for different speed bumps effects . . . . .	25
37	RMS calculations for vertical body acceleration at front, rear and centre of mass . . . . .	25
38	Simulink comparison between the non-optimised and the optimised suspension . . . . .	26

## LIST OF TABLES

1	Car model parameters (Cookson, 2023) . . . . .	4
2	List of tests used to assert the body subsystem. . . . .	5
3	Input parameters ( $[\dot{s}_B, s_B, \dot{s}_W, s_W]$ ) combinations used to assert the suspension subsystem. . . . .	8
4	List of tests used to assert the tyre subsystem. . . . .	9
5	List of tests used to assert the complete model. . . . .	11
6	Sinusoidal road testing parameters . . . . .	15
7	Speed bump testing parameters . . . . .	18
8	Original and optimised car model parameters . . . . .	21

## 1. INTRODUCTION

Road vehicles such as cars use a suspension system to improve performance and comfort. A suspension effectively separates the wheels vertical movement from the body. Most cars implement independent suspensions for each wheel, for ease of computation only one side, or two wheels, are considered hereafter.

Section 2. of this report goes through the steps to implement and test the half-car model shown in Figure 2. The model is constructed in MATLAB's Simulink using a series of subsystem blocks to resolve the body movement given by Equation 1 and Equation 2. All diagrams created can be found in Appendix A.

After the diagrams are proven to work correctly, in Section 3. the model is applied to a real world scenario: driving over a speed bump. The main purpose of installation of these traffic road devices is to reduce speed and volume of traffic to acceptable limits in order to enhance safety for pedestrians and motorists (Shwaly, Zakaria and Al-Ayaat, 2018). Investigation of car behaviour can be important in suspension design as speed bumps have different effects for each vehicle using the road.

Different speed bump shapes, such as the one in Figure 1, can be tested and the optimal suspension for passenger comfort can be found.



**Figure 1.** Speed bump integrated with pedestrian crossing (Brancquart, 2017).

This problem takes into account the vertical motion and the pitch of the car chassis; while the roll is ignored due to simplified nature of the model.

$$m_B \ddot{s}_B = F_{front} + F_{rear} - m_B g \quad (1)$$

$$I \ddot{\theta} = aF_{front} - bF_{rear} \quad (2)$$

## 2. MODEL CONSTRUCTION AND VERIFICATION

The half-car model used is shown in Figure 2, this includes body, suspension and wheel for the front and back of the vehicle. For the purposes of testing and simulation some parameters for this vehicle are chosen and listed in Table 1.

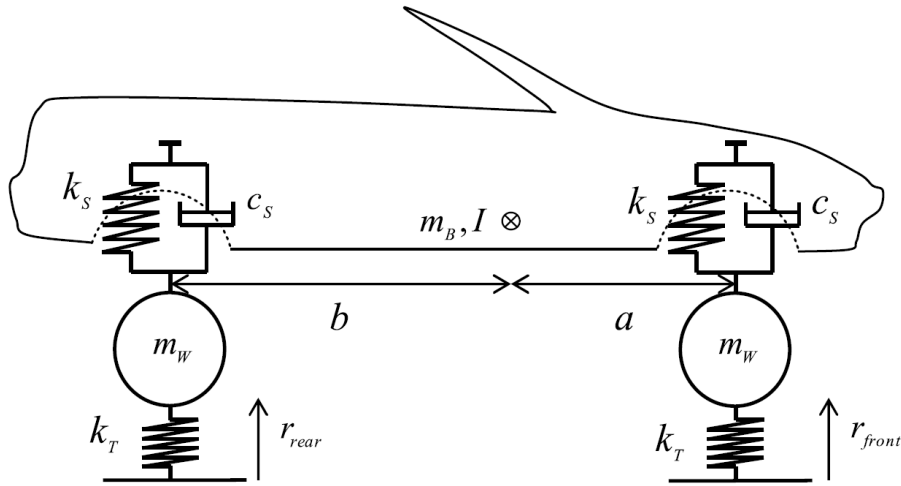


**Figure 2.** Representation of a half-car with two suspensions (Cookson, 2023).

**Table 1.** Car model parameters (Cookson, 2023)

Parameter	Description	Value
$m_W$	Wheel mass	$20\text{kg}$
$k_T$	Wheel stiffness	$14 \times 10^4 \text{Nm}^{-1}$
$k_S$	Spring stiffness	$2 \times 10^4 \text{Nm}^{-1}$
$c_S$	Bumping rate contraction and extension	$[600, 1200]\text{Nsm}^{-1}$
$k_{Sstiff}$	Spring hardening	$20 * k_S$
$m_B$	Body mass	$700\text{kg}$
$I$	Body inertia	$650\text{kgm}^{-2}$
$a$	Front wheel distance from CoG	$1.35\text{m}$
$b$	Rear wheel distance from CoG	$1.5\text{m}$

A free body diagram is created for the model and by applying Newton's Second Law the forces and moments are resolved resulting in the above Equations 1 and 2.

Where  $\ddot{s}_B$  and  $\ddot{\theta}$  are respectively the vertical and angular acceleration of the body.

The equations are further developed to solve the kinematics at each suspension resulting for displacement in:

$$s_{Bf} = s_B + a\theta \quad s_{Br} = s_B - b\theta \quad (3)$$

The equations above are implemented through simulink block models arranged in subsystems for the body, suspension and wheel. These can be found in the library file *CarModelLibrary.slx*.

### 1. Body Model

The half-car body model, shown in the icon block in Figure 3, was implemented in Simulink using the subsystem illustrated in Figure 28. This subsystem produces outputs for linear and angular kinematics, along with the single suspension points.

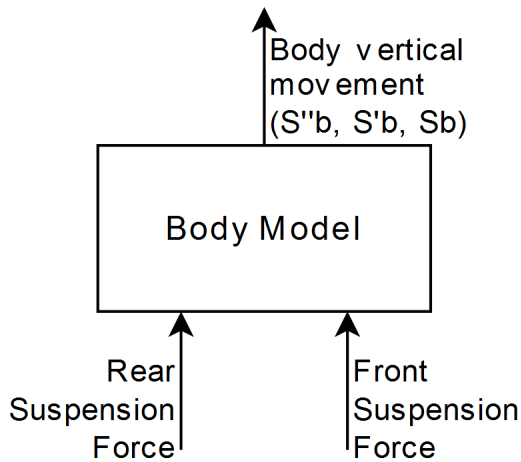


**Figure 3.** Half-Car body icon block.

A series of tests were performed (Figure 31) to verify the correctness of the subsystem, these are listed in Table 2.

**Table 2.** List of tests used to assert the body subsystem.

Type	Description	Expected Result
Free Fall	No force applied to the body ( $F_f \& F_r = 0$ )	Free fall due to gravity, with acceleration equal to $g$ , velocity linearly decreasing and displacement negative parabolic trajectory
Force Equilibrium	Total force applied to body is equal to body weight ( $F_f + F_r = m_B g$ )	According to Newton's First Law when the forces cancel out there is no movement in the body
Lifting Force	Force equal to body weight applied to each suspension ( $F_f \& F_r = m_B g$ )	The resultant force on the body is equal to the weight but points upwards. Similar to the free fall test but this time moving upwards

The free fall test validates the accurate implementation of Equation 1 through the examination of body displacement. With null inputs, the test ensures the accurate calculation of internal forces, such as weight, without external force interference. The result in Figure 4 showcases a parabolic displacement with linear velocity and a constant acceleration equal to ' $g$ '.

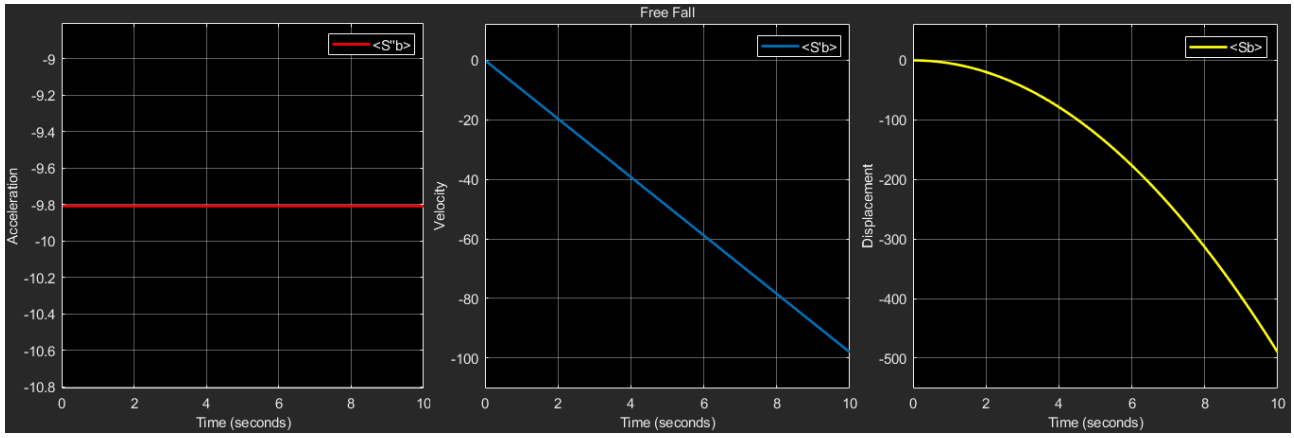


**Figure 4.** Free fall test body movement

The force equilibrium test validates the accurate implementation of Equation 2 by examining the body pitch. The upward force applied to the car is distributed proportionally across the two suspensions to prevent the introduction of any moments around the centre of gravity (CoG). The outcome shown in Figure 5, reveals a pitch of 0, indicating the cancellation of moments through a correct implementation of the free body diagram. It's worth noting that the y-axis was manually scaled to visualise these results, as a pitch angle of approximately  $10^{-14}$  radians was observed. This minute angle is likely attributable to rounding errors, deemed negligible due to its small magnitude, and consequently, the test is considered successful.

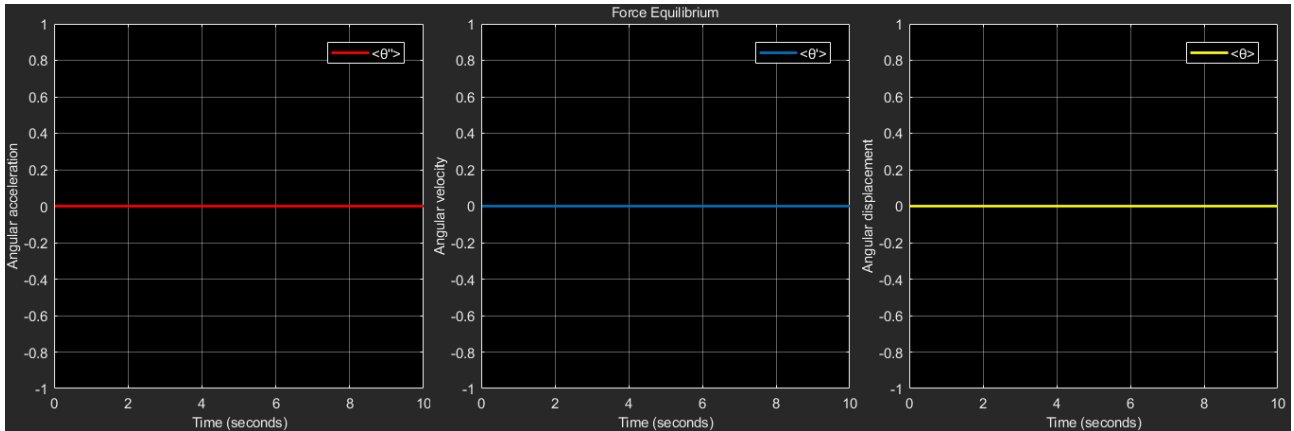


**Figure 5.** Force equilibrium test body pitch

The final test, the lifting force, validates both resultant forces and moments acting together on the body. Solving Equation 1 the output force is equal to the weight but with opposite sign resulting in a displacement similar to free fall but in opposite direction (Figure 6). As the same force is applied to each suspension a moment is induced in the body due to its asymmetry. This results in a downward pitch of the car as the back wheel is further from the CoG (Figure 7).

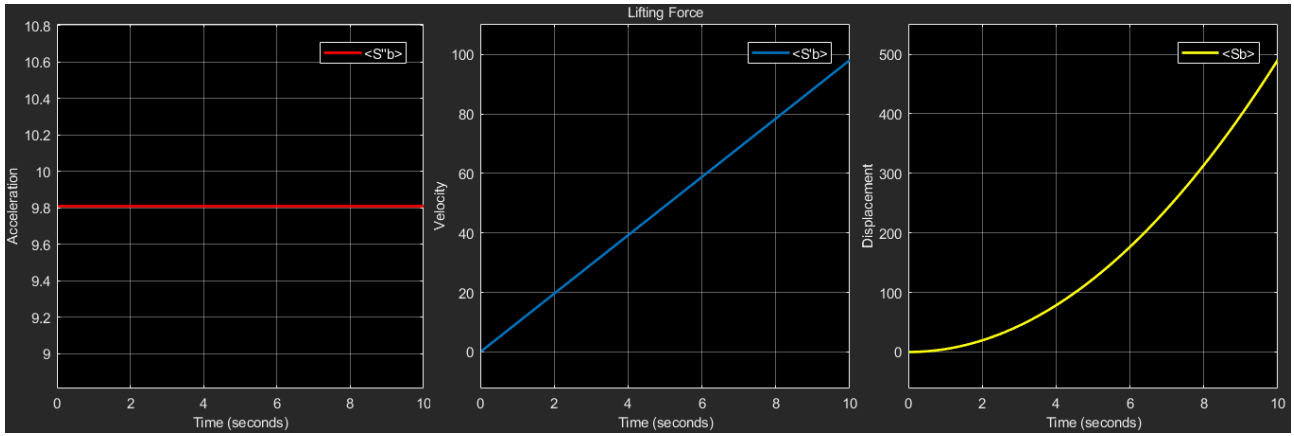


Figure 6. Lifting force test body movement

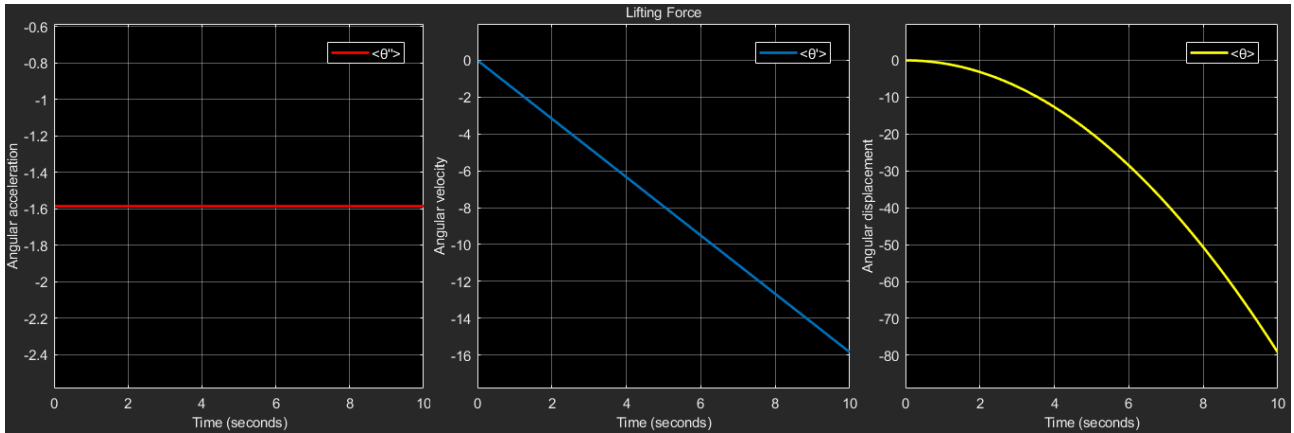


Figure 7. Lifting force test body pitch

## 2. Suspension Model

The half-car suspension model, shown in the icon block in Figure 8, was implemented in Simulink using the subsystem illustrated in Figure 29. This subsystem outputs the single suspension force which will then apply to the body.

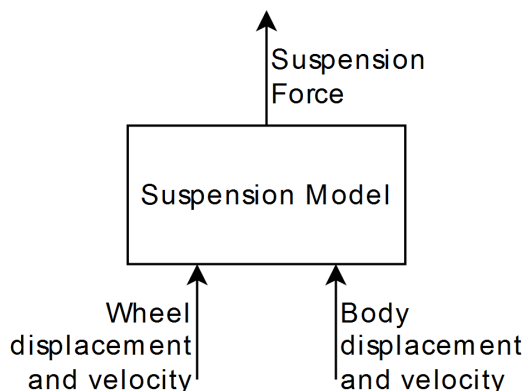


Figure 8. Half-Car suspension icon block.

A car suspension system is made of a spring and a dampener working together to stabilise the car and reduce the impacts (Figure 2). The relationship between the input displacement and velocity and the output force is given by Equation 4.

$$F = k_s(s_B - s_W) + c_S(\dot{s}_B - \dot{s}_W) \quad (4)$$

A direct comparison with the analytical solution was chosen as a suitable test for the suspension subsystem modelled by Equation 4. Six combinations of the input parameters  $[\dot{s}_B, s_B, \dot{s}_W, s_W]$  are listed in Table 3 and the solution was compared using the values in Table 1 (Figure 31).

**Table 3.** Input parameters ( $[\dot{s}_B, s_B, \dot{s}_W, s_W]$ ) combinations used to assert the suspension subsystem.

Inputs	Expected Solution
[0, 0, 0, 0]	0
[0, 0, 0, 1]	20000
[0, 0, 1, 1]	20900
[0, 1, 0, 0]	-20000
[1, 1, 0, 0]	-20900
[1, 1, 1, 1]	0

### 3. Wheel Model

The half-car wheel model, shown in the icon block in Figure 9, was implemented in Simulink using the subsystem illustrated in Figure 30. This subsystem produces outputs for linear displacement and velocity of the wheel.

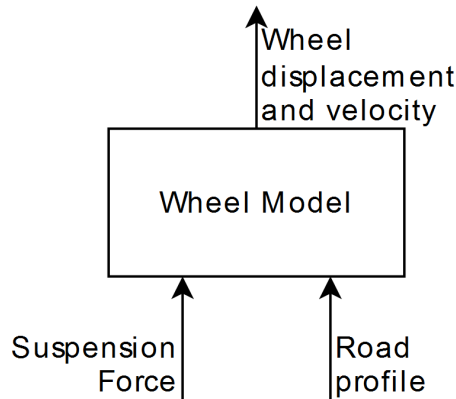


**Figure 9.** Half-Car wheel icon block.

From the free body diagram of the wheel the sum of all the forces is given by Equation 5. The displacement and velocity can be obtained by integrating the acceleration.

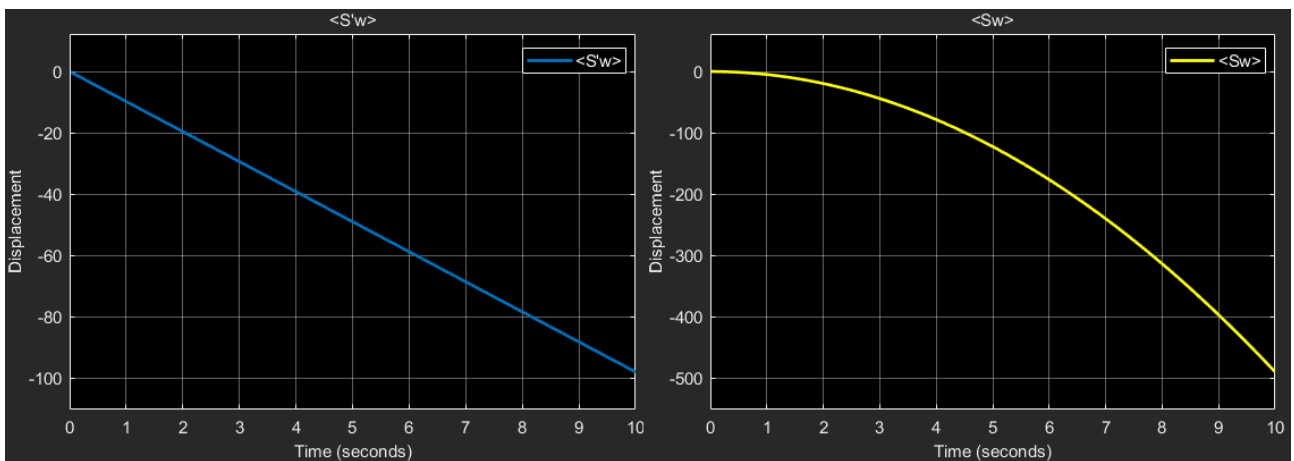
$$m_W \ddot{s}_w = -F + k_T(r - s_W) - m_W g \quad (5)$$

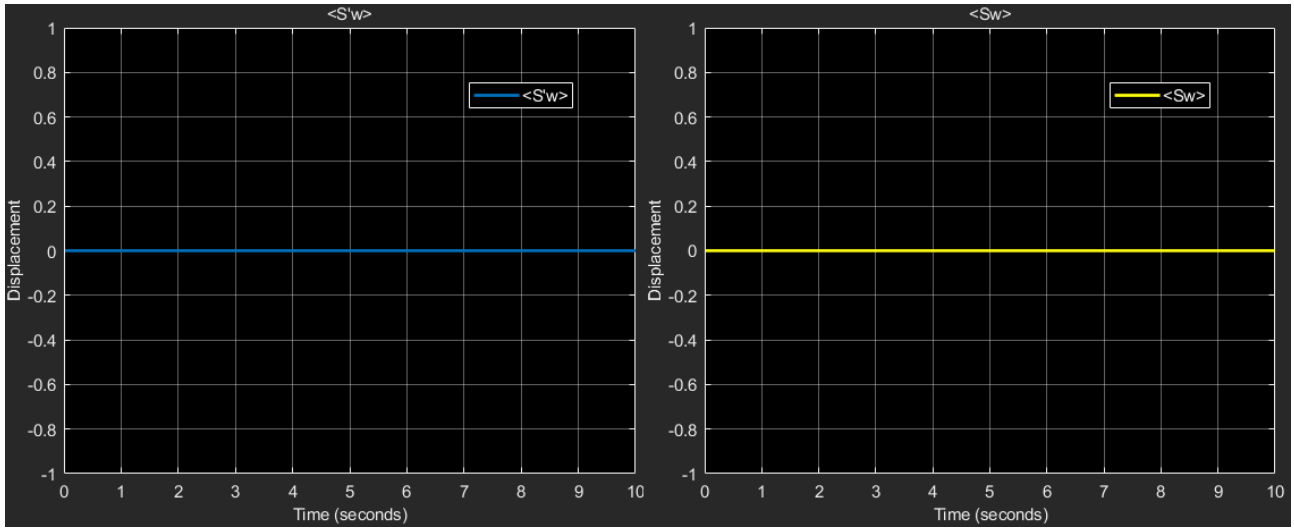
A series of tests were performed (Figure 31) to verify the correctness of the subsystem, these are listed in Table 4.

**Table 4.** List of tests used to assert the tyre subsystem.

Type	Description	Expected Result
Free Fall	No suspension force applied to the wheel and no tyre stiffness ( $F = 0, k_T = 0$ )	Free fall due to gravity, with velocity linearly decreasing and displacement negative parabolic trajectory
Force Equilibrium	Total force applied to tyre is equal to tyre weight and no tyre stiffness ( $F = m_W g, k_T = 0$ )	According to Newton's First Law when the forces cancel out there is no movement in the body
Road Step	Step input as road surface with no suspension force nor gravity ( $F = 0, g = 0$ )	Constant oscillation of displacement and velocity with frequency= $\sqrt{k_T/m_W}$

The free fall and force equilibrium test validates the accurate implementation of Equation 5 through the examination of body displacement. With null inputs, the test ensures the accurate calculation of internal forces, such as weight, without external force interference. With the resultant force equal to zero the tyre is in equilibrium, with no vertical displacement nor velocity. The results in Figures 10 and 11 showcases a constant acceleration equal to 'g' in the former and no movement in the latter.

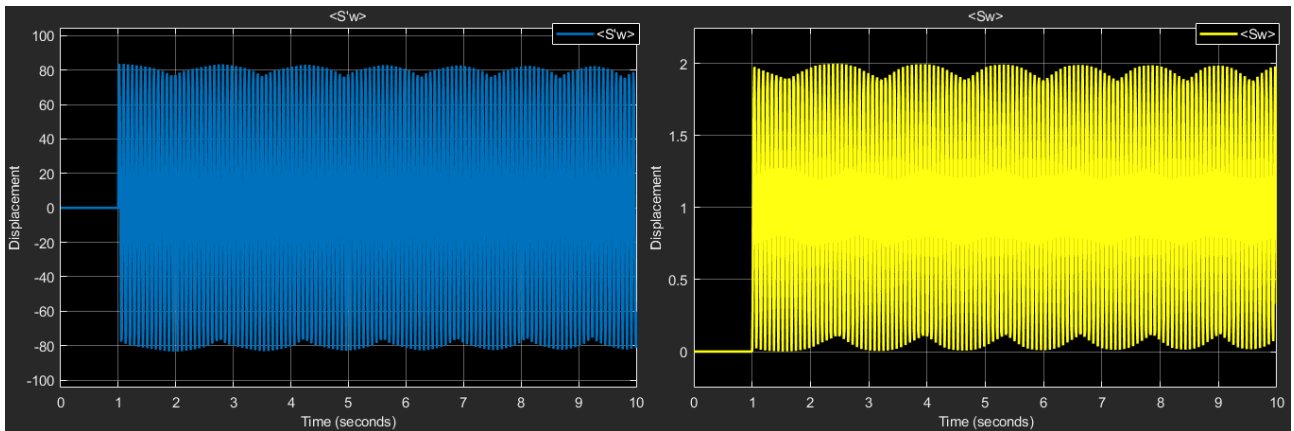
**Figure 10.** Free fall test wheel movement



**Figure 11.** Force equilibrium test wheel

The final test, the road step, validates the third component of the equation: the spring like tyre. With the remaining terms as 0, the output movement is only given by the spring response. When a road step is applied the spring starts oscillating at its natural frequency and due to the lack of other forces the oscillation continues indefinitely (Figure 12).

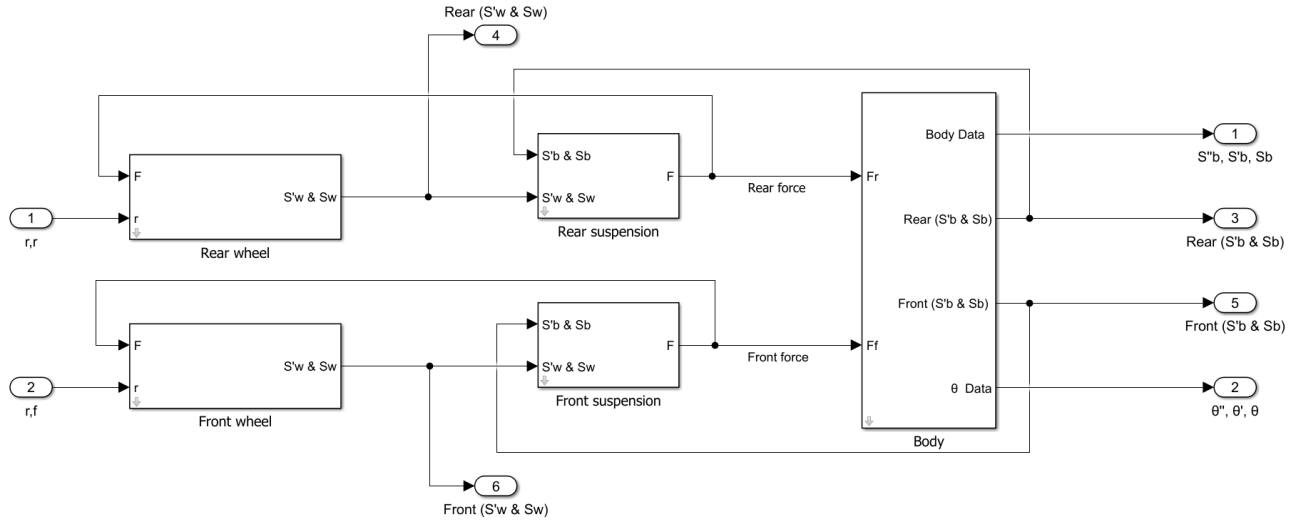
The natural frequency in Hertz of the spring is given by  $f = \frac{\sqrt{k_T/m_W}}{2\pi}$ , using the values in Table 1 this gives a value of  $13.3159\text{Hz}$ . Using cursors in Figure 12 the frequency, using the period, was measured at  $13.3321\text{Hz}$  proving the correct implementation of the wheel subsystem.



**Figure 12.** Road step test wheel movement

#### 4. Complete half-car Model

Finally, the complete half-car model can be implemented in Simulink by assembling the single subsystems and connecting the relative inputs and outputs. The half-car model, shown in Figure 13, is a combination of the subsystems for both the front and rear wheel and suspensions. The model takes the road surface as input and outputs a series of data relevant to the car kinematics, including vertical and pitch movements.

**Figure 13.** Half-Car model assembly.

A series of tests were performed (Figure 32) to verify the correctness of the complete model, these are listed in Table 5.

**Table 5.** List of tests used to assert the complete model.

Type	Description	Expected Result
Stationary	No road input ( $r = 0$ )	The system is only subject to gravity, the suspension and wheel are compressed under the car weight and should soon settle
Suspension Test	Road step input and rigid wheel with $k_T$ very high and $m_W$ very low allows to remove the wheel	The system starts oscillating due to the road and settle soon after.
Wheel Test	Road step input and rigid suspension with $k_S$ and $c_S$ very high allows to remove the suspension	The system starts oscillating due to the road and keeps the osculation due to a lack of external forces.
Non-Linear comparison	Introduce non-linear parameters in springs and dampener and compare it to the linear outputs	Differences in periods and amplitudes of the oscillations.
Non-Linear step input	Observe body movement under a step road with non-linear parameters	Wheel bouncing on the ground proving correct behaviour

The stationary test investigates the body movement on a flat road. When the simulation is started the suspension is unloaded therefore the weight of the car is the first force acting on the system. This causes both the wheel and the suspension to compress and oscillate. As the road surface is constantly 0, the system soon stabilises and the body reaches an equilibrium roughly 20cm below the initial position (Figure 14).

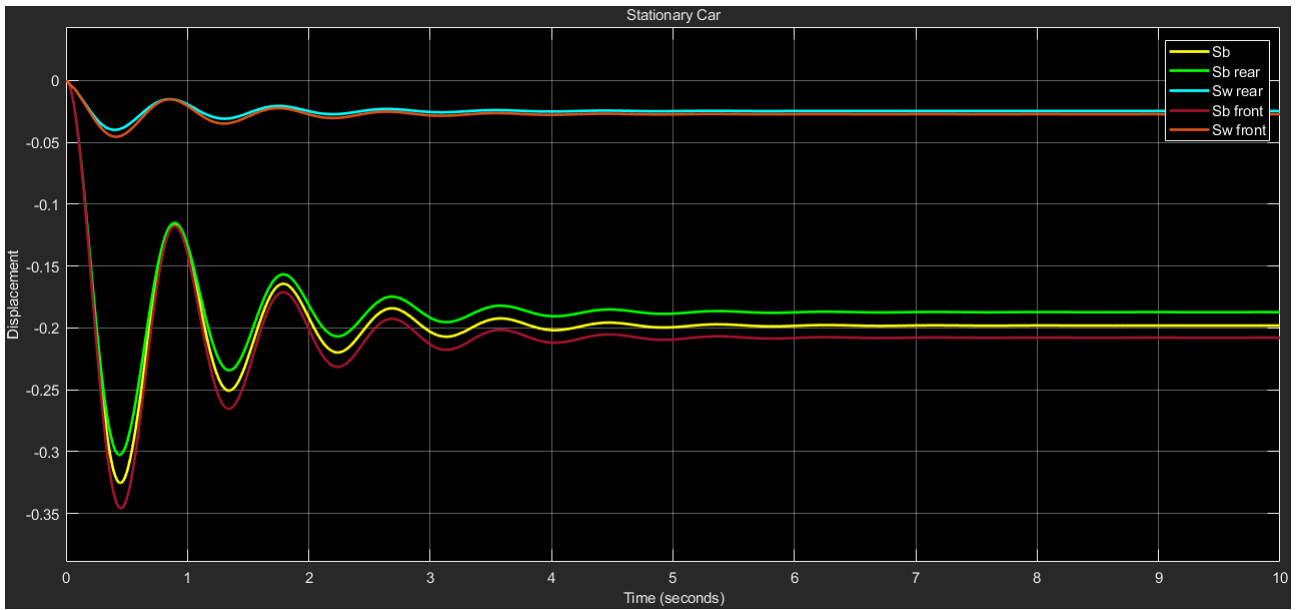


**Figure 14.** Stationary car test body and wheel movement

The suspension and wheel tests investigate the body movement under a step input road respectively when the wheel or the suspension are disabled. To make the wheel rigid the stiffness is increased by a factor of  $10^4$  while the mass is decreased by the same factor. The result in Figure 15 illustrates the oscillation given by the suspension spring and the stabilisation resulting from the suspension dampener. To make the suspension rigid the stiffness and dampening coefficients are increased by a factor of  $10^6$ . The result in Figure 16 illustrates the oscillation given by the wheel springiness, due to a lack of dampening this oscillation continues indefinitely. In addition it can be observed the negligible suspension movement as the body and the wheel masses act as a single rigid body.

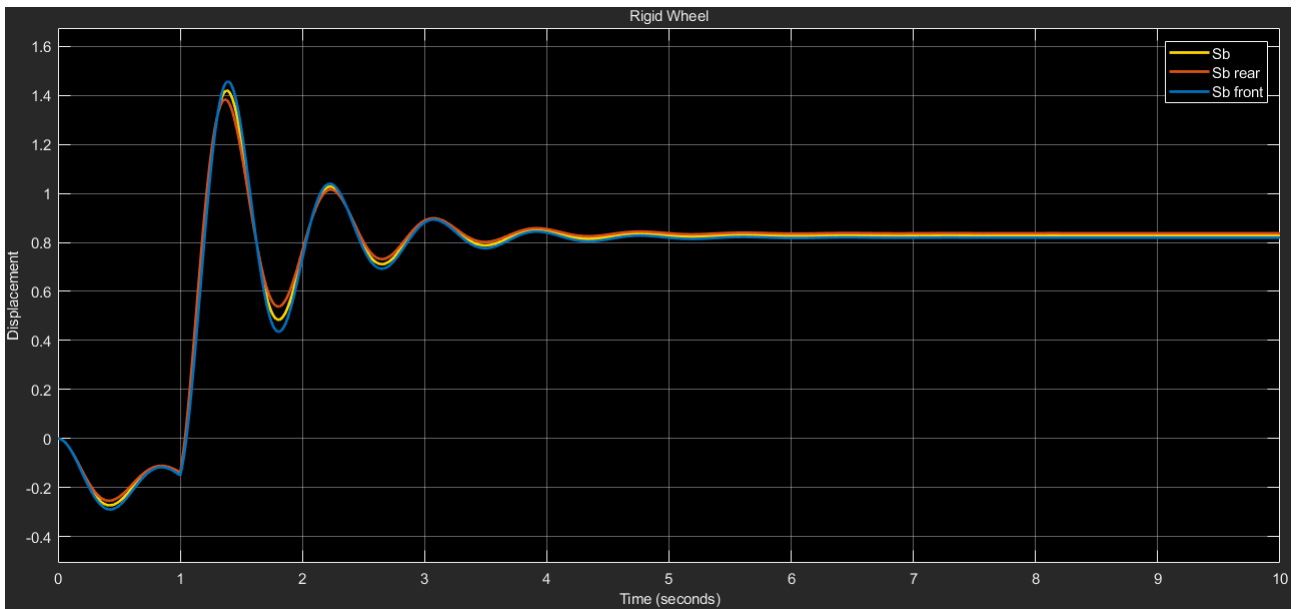


**Figure 15.** Road step test body movement with a rigid wheel

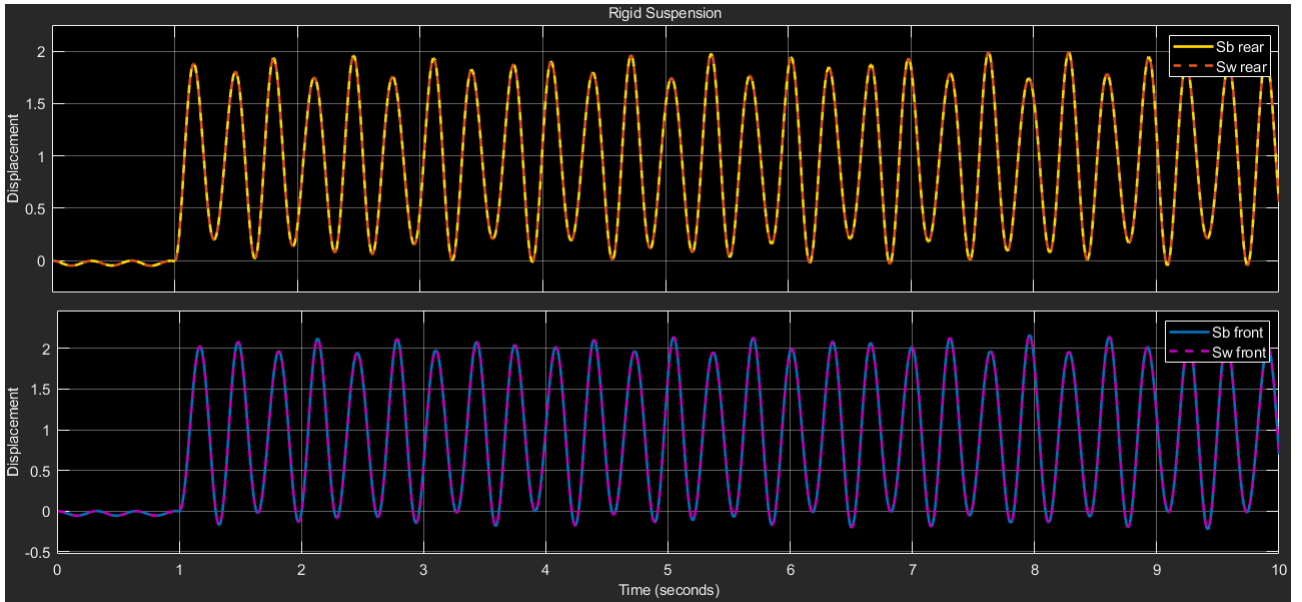


**Figure 16.** Road step test body and wheel movement with a rigid suspension

So far all tests were conducted with linear parameters for the springs and the dampener. This meant that the springs behaved linearly no matter the elongation while the dampener ignored the compression or extension phase. To better represent real world behaviour the spring hardening and the different damping rates are introduced. The spring hardening curve is given by Figure 17; the damping rates, which were previously averaged, are given in Table 1.

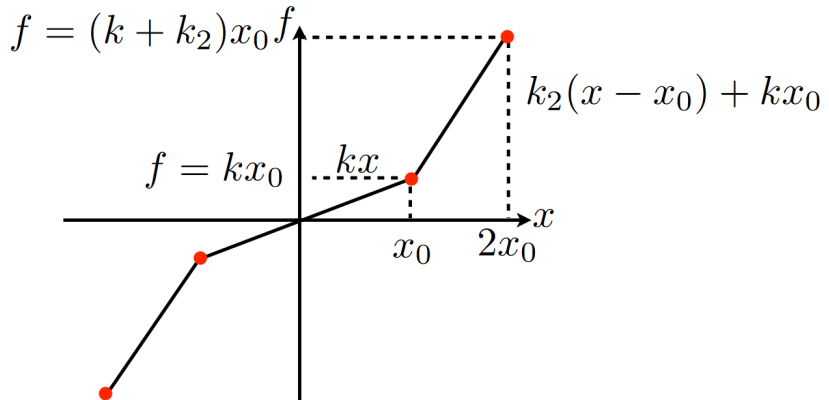


**Figure 17.** Suspension spring non-linear coefficient

The first non-linear test is a direct comparison with the linear one. The same stationary conditions of the previous test were applied and the results compared in Figure 18. The result shows the correct implementation of the non-linear parameters through look-up tables as the same equilibrium is reached.

To major effects, noticed with the implantation of non-linearities, is a change in amplitude and in period. The amplitude is observed to decrease in one direction while increasing in the other, this is because the new damping coefficients are larger for extension and smaller for compression.

The increase in frequency is due to the larger spring coefficient. The car mostly oscillates in a range above the hardening limit ( $x_0$ ) increasing  $k_S$ . A higher coefficient gives a higher frequency due to the relationship  $f = \frac{\sqrt{2k_S/m_B}}{2\pi}$ .

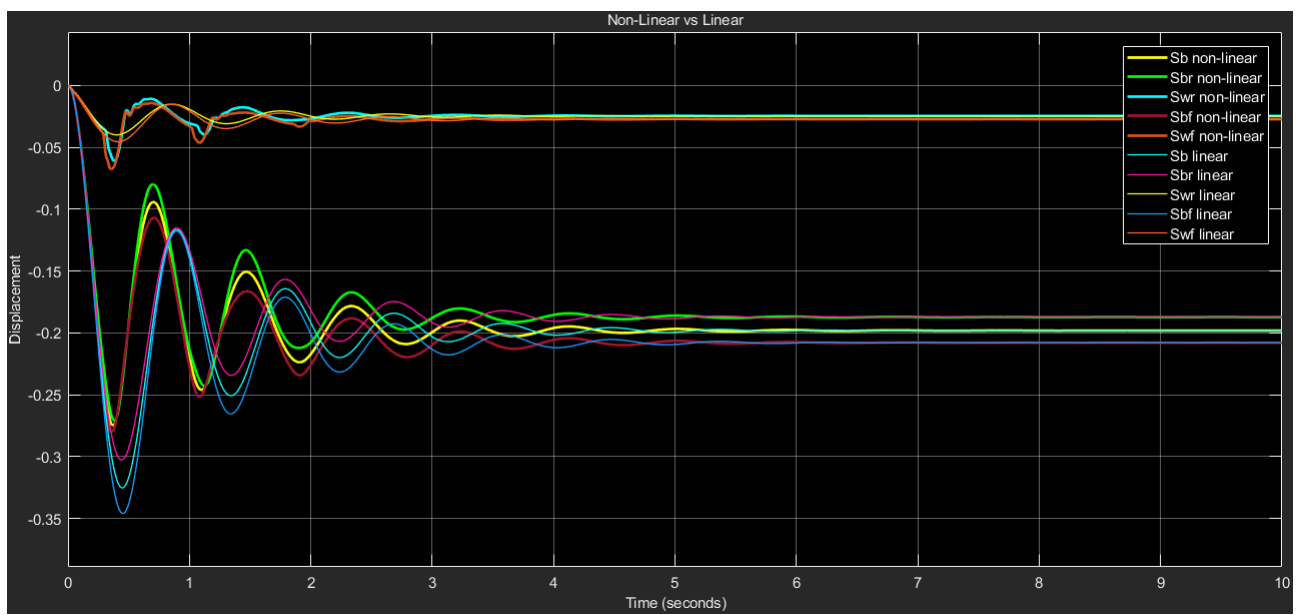


**Figure 18.** Non-linear comparison on a stationary car test showing body and wheel movement

The last test is the application of a road step input To the non-linear model. By introducing a non linear tyre stiffness the idealised constant contact with ground is removed and the wheel is allowed to lift off. When plotting the body displacement in Figure 19 a series of large bounces are observed as the result of the 1m step. The wheel correctly detaches from the ground and falls back due to gravity until it stabilises due to the suspension dampening.

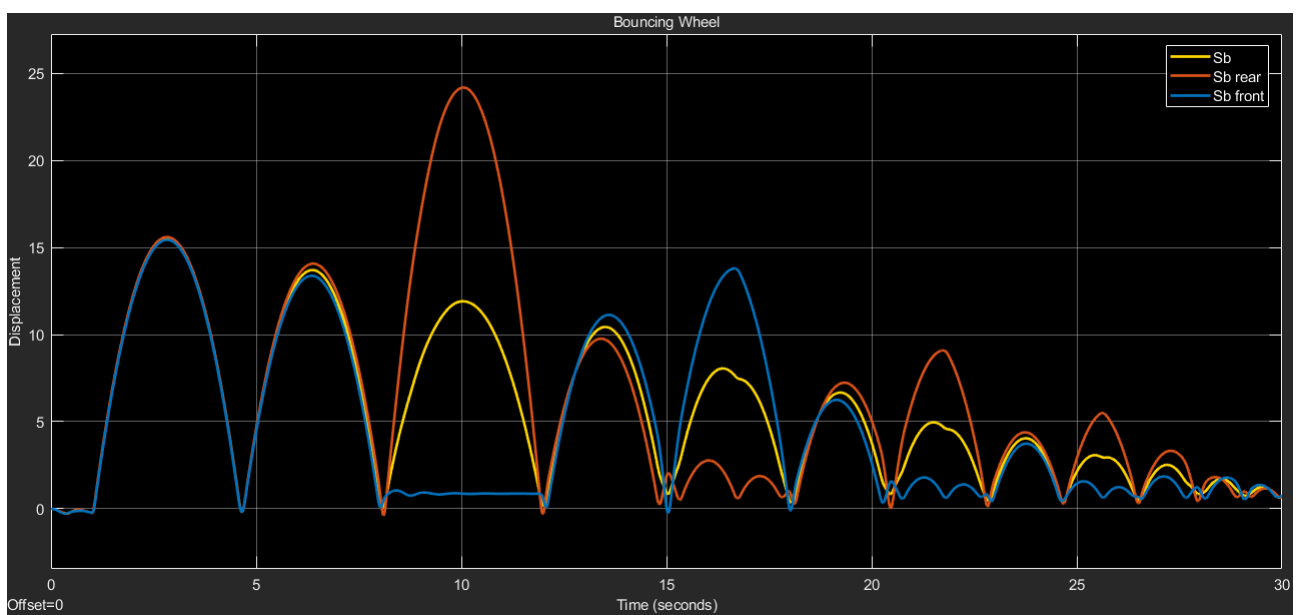


**Figure 19.** Road step test body movement with non-linear parameters

### 3. INVESTIGATION OF CAR PERFORMANCE

Once the model is constructed and its performance is verified it can then be applied to a real road scenario. The constructed car is driven over two road conditions to analyse its performance and optimise the suspension characteristics improving passenger safety and comfort.

#### 1. Sinusoidal Road

The first road condition is a perfect sinusoidal road. Despite this is rarely the case in a real world scenario its a first step in the simulation process. The road input 'r' is consequently given by:

$$r = A \sin 2\pi f t \quad (6)$$

where,  $A$  is the amplitude in metres,  $f$  is the sinusoidal frequency ( $v/\lambda$ ) and  $t$  the time in seconds. As the car is assumed to drive forward a phase lag is introduced in the back wheel equal to  $\phi = 2\pi \frac{(a+b)}{\lambda}$ . A range of car velocities and road amplitudes were tested (Figure 33) and reported in Table 6, while the wavelength was fixed at 1m.

**Table 6.** Sinusoidal road testing parameters

Parameter	Description	Value
$v$	Car velocity	$[1, 2, 3, 5, 8, 10] ms^{-1}$
$A$	Road amplitude	$[0.01, 0.05, 0.1] m$
$\lambda$	Road wavelength	1m

The initial test consists in analysing the effect of vehicle speed on the system. The road amplitude was fixed to  $A = 0.01m$  while the range of velocity was used. The results in Figure 20 illustrates the initial oscillation due to the car weight applied to the unloaded suspensions and tyres and, subsequently, the oscillation induced by the road.

All velocities roughly converge to the same value despite the variation in amplitude and frequency. These variations are direct consequence of the speed as the faster the car travels the more bumps it encounters per unit time. The highest velocity ( $10ms^{-1}$ ) while producing the smallest displacement it also has the highest body jerk which may negatively impact passenger comfort. Higher velocities where not tested as a trend could already be extracted from this range, those would give increasingly smaller displacements while also increasing the jerk.

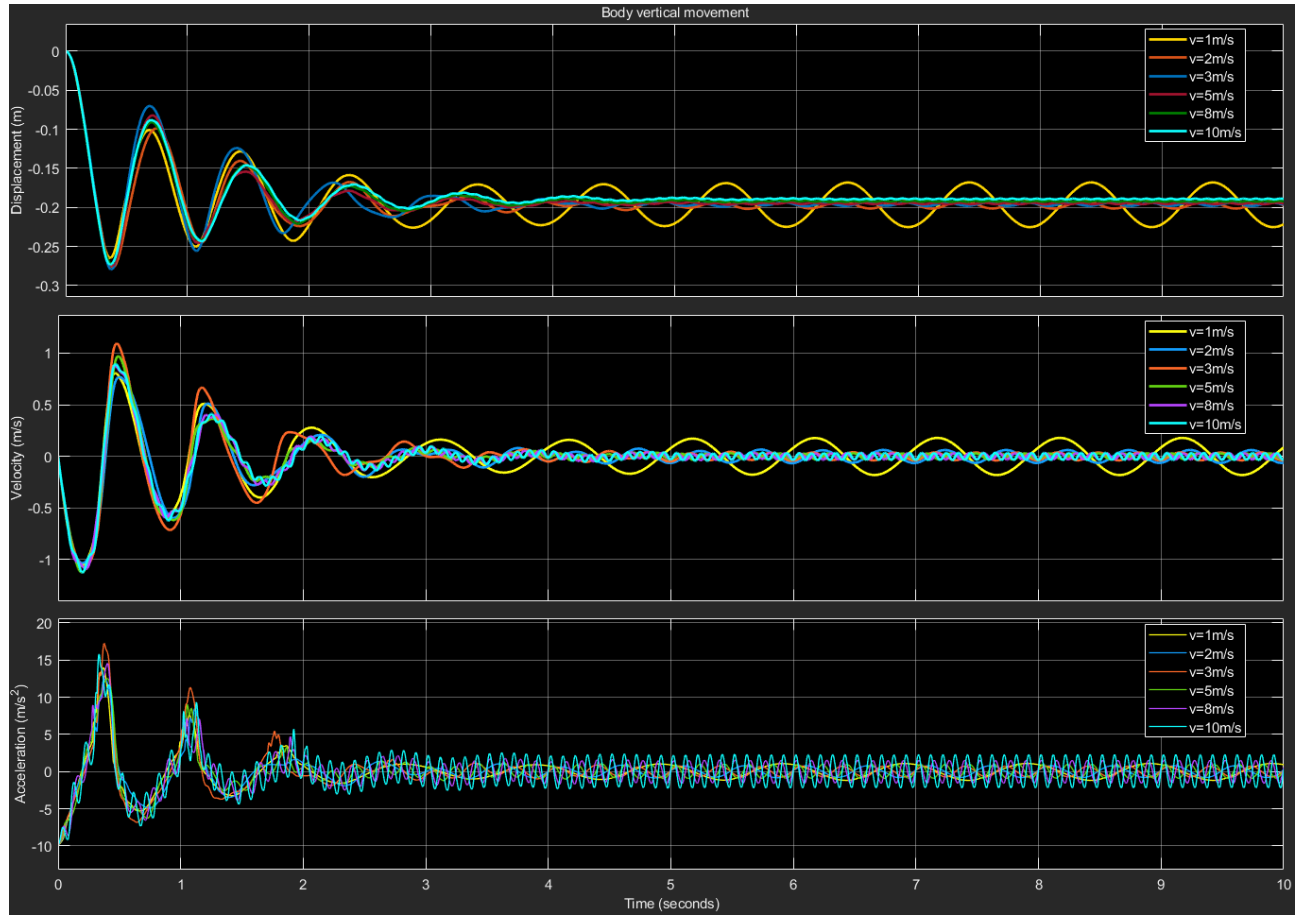


**Figure 20.** Sinusoidal road test body movement with amplitude  $A = 0.01m$

The second test consists in analysing the effect of road amplitude on the system. The vehicle speed was fixed to  $v = 10ms^{-1}$  while the range of amplitudes was used.

The results in Figure 21 illustrates a similar behaviour between the first two amplitudes only showing a slight decrease in displacement and frequency of oscillation. On the other hand the 10cm amplitude shows major effects on the car body which does not stabilise within reasonable time. The body displacement is high and the wheels are very close to detaching from the ground causing an infinite oscillation. The large displacements also cause high jerk decreasing passenger comfort.

The range of amplitudes was selected with increases of 5cm as, smaller increments wouldn't result in significant variations in the expected results.

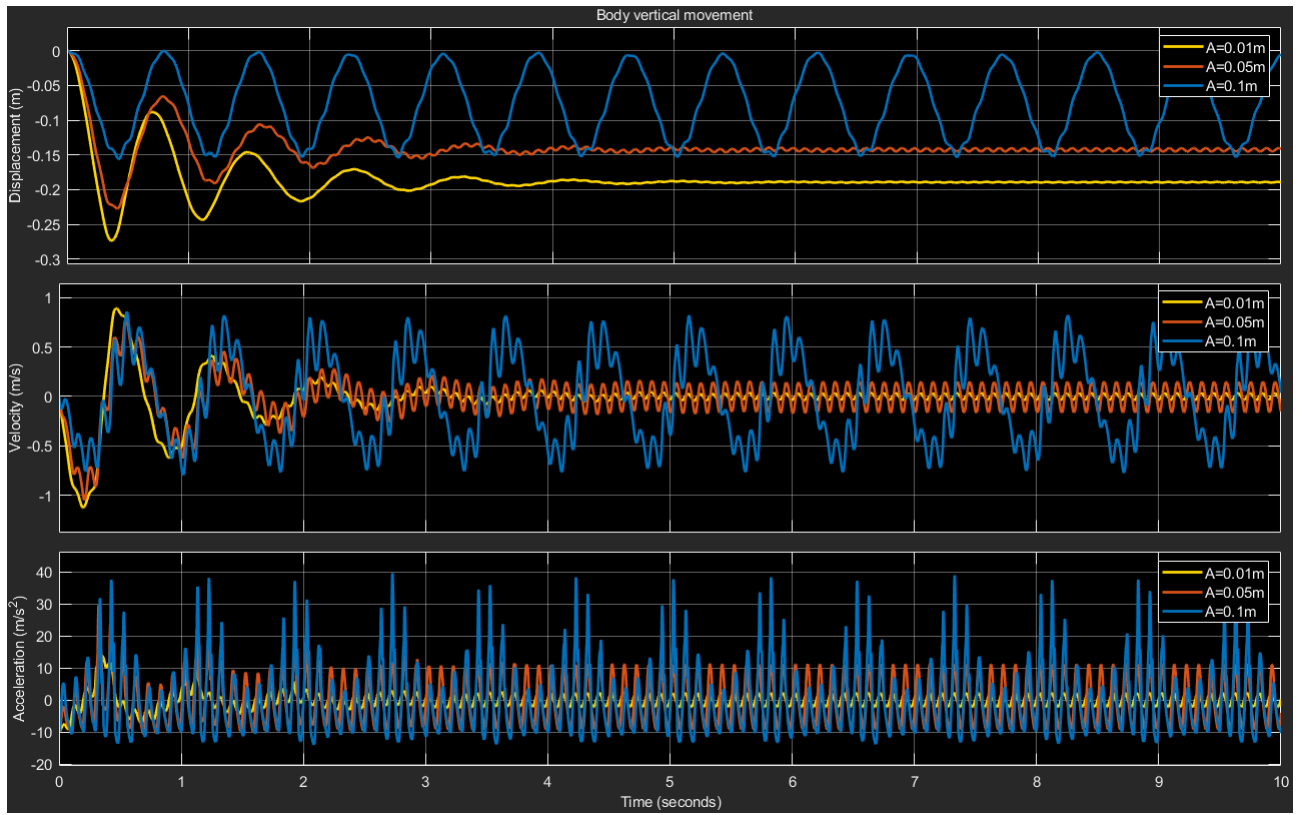


**Figure 21.** Sinusoidal road test body movement with velocity  $v = 10ms^{-1}$

## 2. Speed Bump

The final road condition is a speed bump. These are traffic calming devices installed on roads to reduce vehicle speeds. Speed bumps work by acting on the wheels, changing the vehicle vertical movements resulting in increased passenger discomfort. As the discomfort increases with vehicle speed the driver tends to slow down in proximity of speed bumps (Antić et al., 2013).

**2.a. Car Behaviour** Two speed bumps are defined: a Watts profile and a Seminole profile shown in Figure 22.

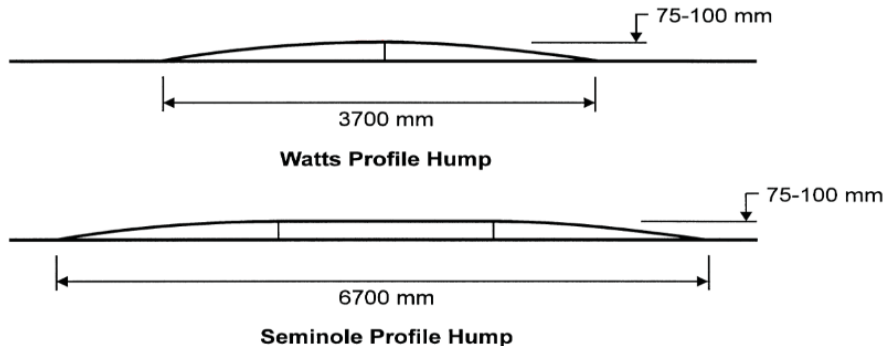


**Figure 22.** Watts and Seminole profile speed bumps (Shwaly, Zakaria and Al-Ayaat, 2018)

The Watts profile was modelled with a simple window around a sinusoidal road to only extract one bump. The Seminole profile instead starts with the Watts profile and adds a flat constant section at the peak. The two bumps are tested in Figure 36 with the parameters given in Table 7.

**Table 7.** Speed bump testing parameters

Parameter	Description	Value
$h$	Bump height	0.1m
$L$	Watts bump length	3.7m
$d$	Seminole top surface length	3m
$v$	Car velocity	$8ms^{-1}(28.8km/h)$

The result of driving over a Watts bump is shown in Figure 23. After the usual initial oscillation due the suspensions compression, the car stabilises and around 5.5 seconds into the simulation hits the bump. The front suspension is affected first while the rear has a lag due to the inter-axis distance. While the body vertical movement is uniform a moment in the car is generated resulting in an oscillation of the pitch. This can be noticed by the rear wheel moving down when the front wheel hits the bump, before moving back up when itself reaches the bump.

It can also be noticed how the single wheels move by the bump height while the car is only displaced by less than half. An ideal suspension would only move the wheel while the car body is stationary.

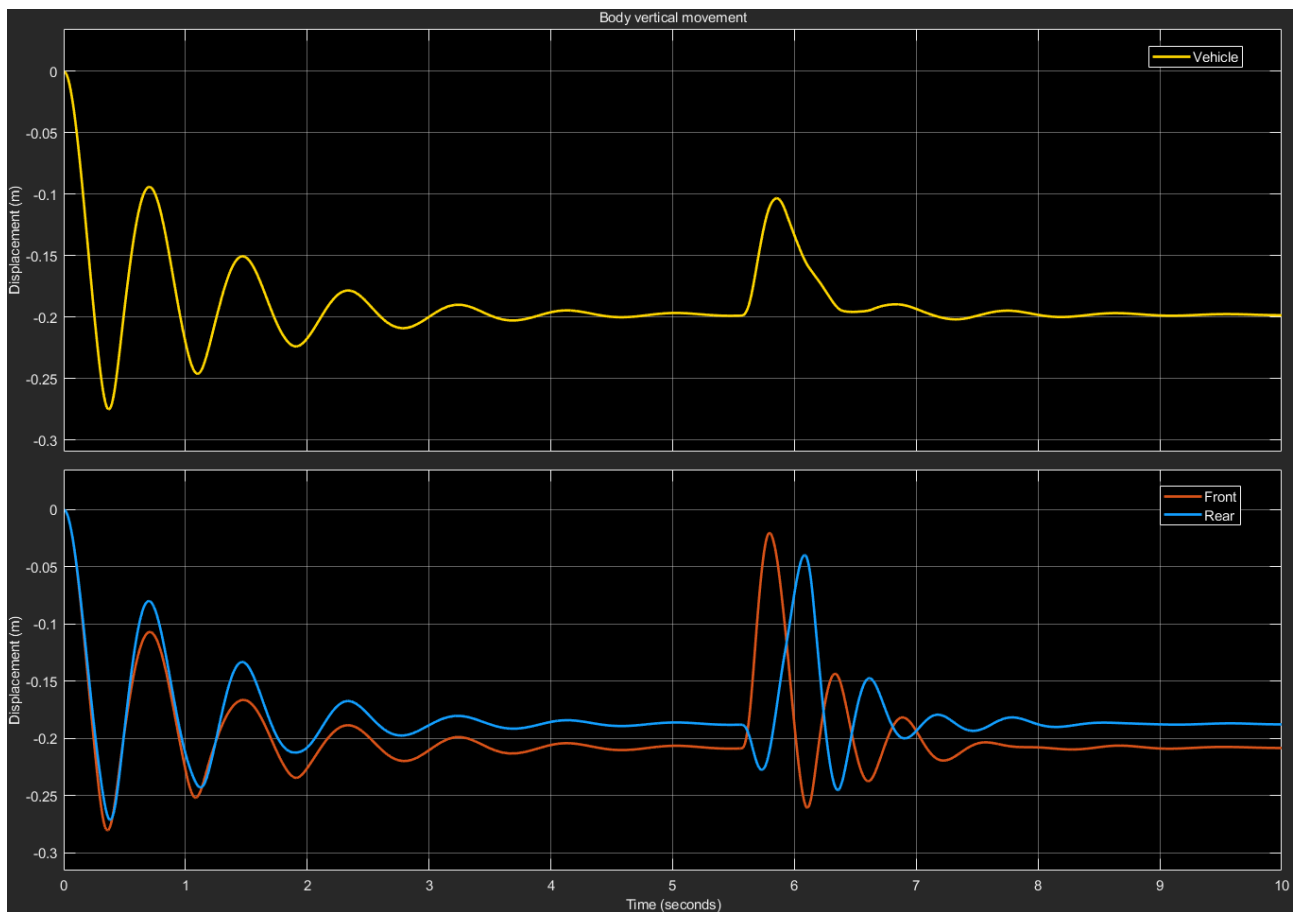


**Figure 23.** Car movement while driving at  $8m/s$  over a single Watts profile speed bump around 5.5s

The Seminole profile bump has a very similar effect shown in Figure 24. This time though the top flat surface is long enough for the car to stabilise before descending the bump.

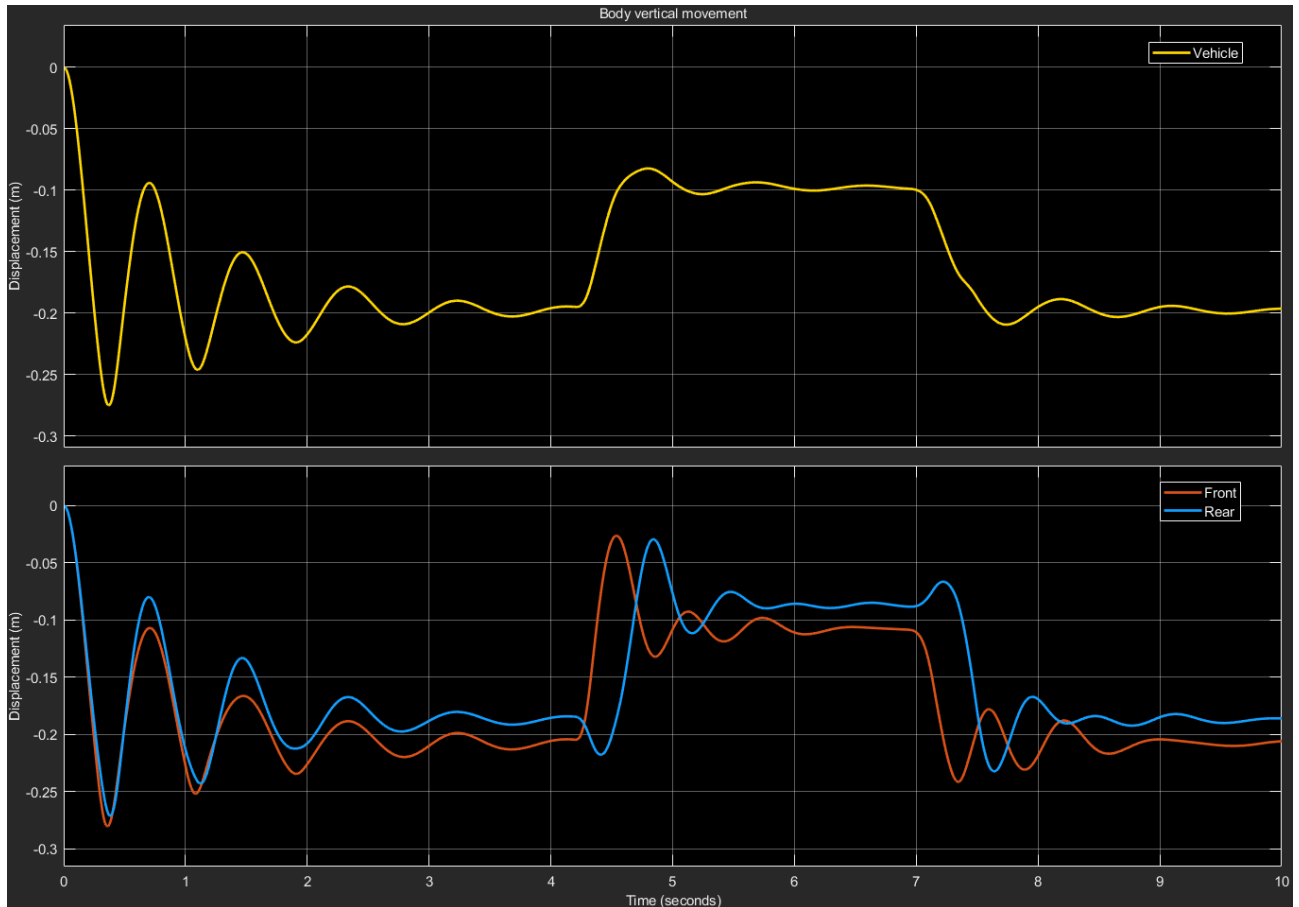


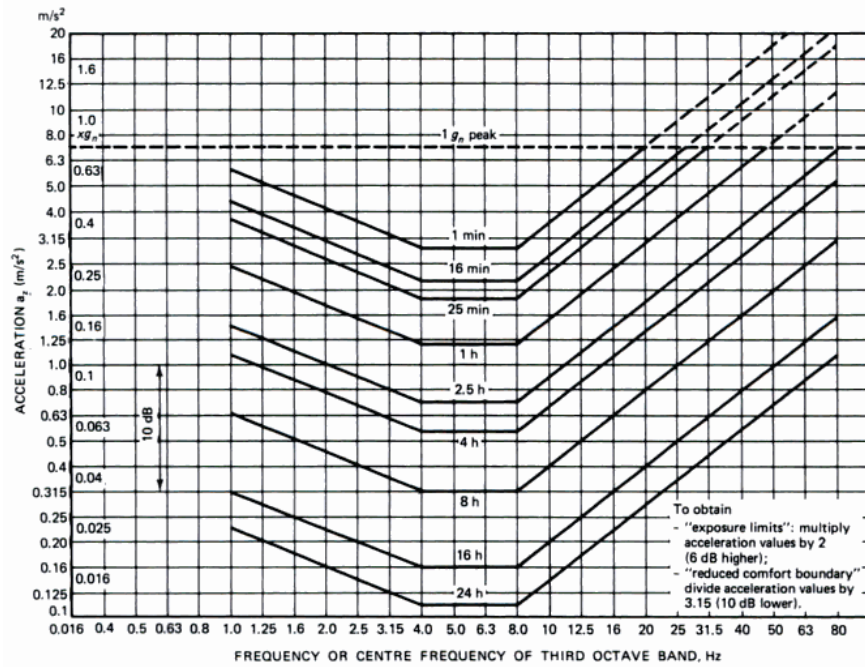
**Figure 24.** Car movement while driving at 8m/s over a single Seminole profile speed bump around 4.3s

With this, it can be noted how the effect of a speed bump on a car is highly dependent on the bump height and the car velocity. For the given conditions the speed bump has a significant effect on the body and wheel movement. The front wheel is close to reaching the zero displacement value, which if surpassed would mean the wheel has detached from the ground. The Seminole profile has a greater effect on the vehicle as it effectively disturbs the suspension twice increasing the overall oscillation time. These speed bumps would be useful in enforcing a 30km/h speed limit as any higher speed would result in a tyre liftoff and therefore increase passenger discomfort.

**2.b. Passenger Comfort Optimisation** During the design of a vehicle, suspension optimisations is used to investigate the best parameters for a given response. Usually in car design this response is either the car exposure to vibrations or the passenger comfort.

In this report a demonstration is given for the improvement of passenger comfort over a predefined speed bump, optimising the spring and dampener coefficients. During the optimisation the car weight and centre of mass were assumed to be invariant as the car cannot be redesigned just to suite a specific suspension. Additionally, optimising for a specific speed bump is not a univocal solution as the car will eventually be subject to different road conditions.

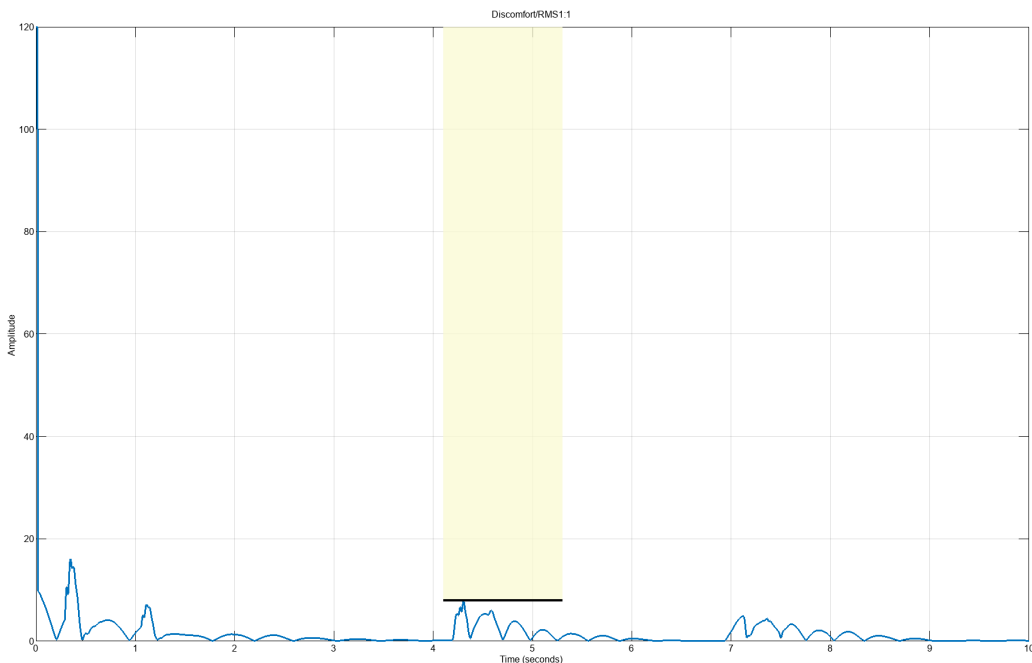
The ISO-2631 standard defines passenger discomfort as the combination of vertical acceleration, frequency of vibration and time of exposure (Figure 25).



**Figure 25.** Human body vertical acceleration exposure limits according to ISO (2018)

In a single speed bump scenario the exposure limit is clearly never reached but comfort can still be improved by reducing the transmitted vertical acceleration. Simulink's optimiser application was used to optimise the spring stiffness and hardening and the dampener contraction and extension coefficients while observing the body RMS acceleration (Figure 37). The car was subject to the same Seminole speed bump as in the previous section, as it displayed the most uncomfortable scenario.

As seen in Figure 26 a solution was found that would minimise the suspension transmitted acceleration during the speed bump event. The optimal parameters found are compared in Table 8 with the original ones.

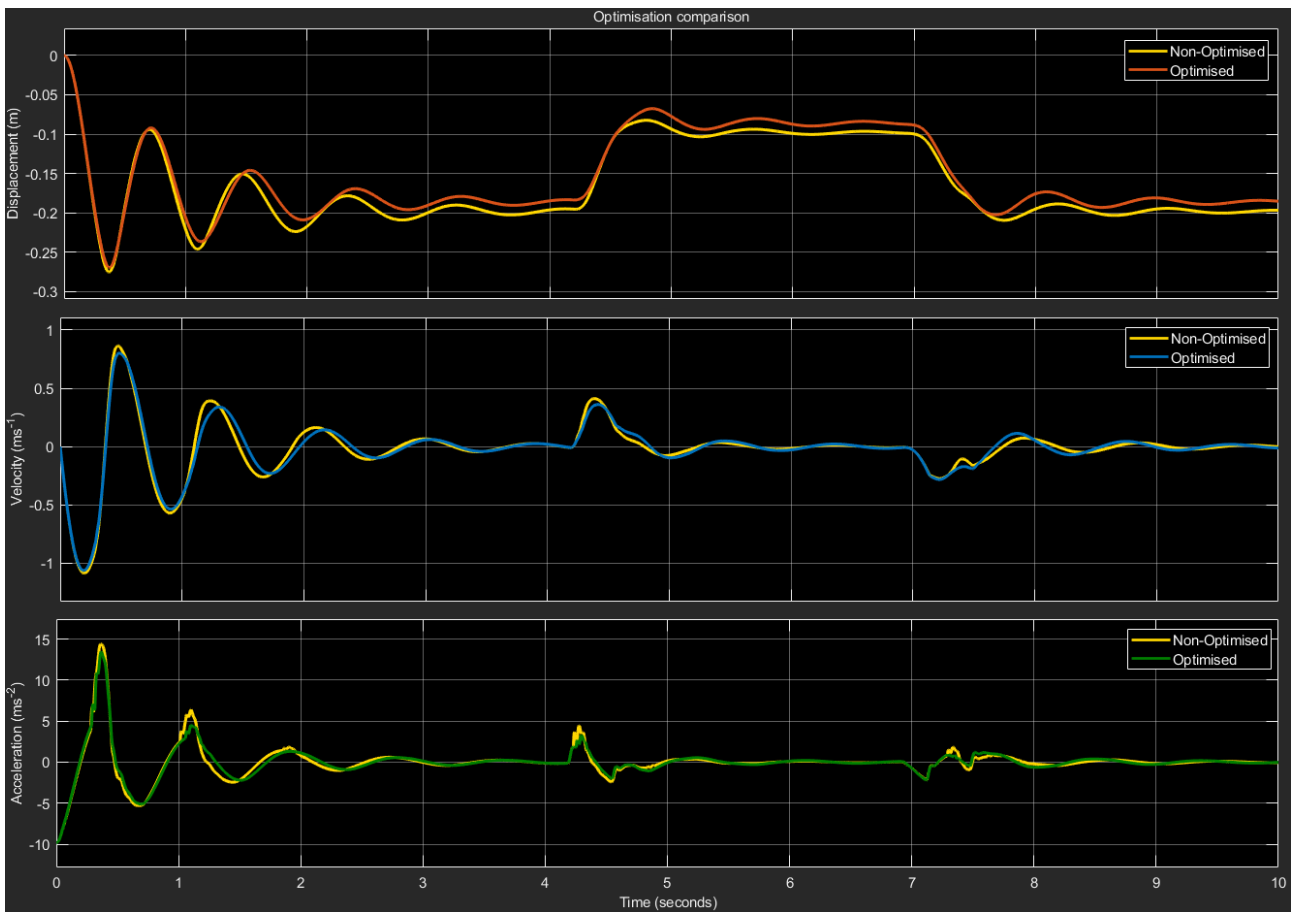


**Figure 26.** Optimisation boundary around the speed bump induced acceleration

**Table 8.** Original and optimised car model parameters

Parameter	Description	Original Value	Optimised Value
$k_S$	Spring stiffness	$2 \times 10^4 Nm^{-1}$	$2.15 \times 10^4 Nm^{-1}$
$c_S$	Bumping rate contraction and extension	$[600, 1200] Nsm^{-1}$	$[600.36, 1210] Nsm^{-1}$
$k_{Sstiff}$	Spring hardening	$20 * k_S$	$19.93 * k_S$

Finally, the optimised parameters, now in the Simulink model, are compared with the original (Figure 27). Figure 27 demonstrated the overall decrease of the event effect on the car body. All three outputs, displacement, velocity and acceleration, show an improvement which in turn means a passenger ride comfort increase.

**Figure 27.** Comparison between the non-optimised and optimised suspensions on the car body movement

The improvement is relatively small but this is to be expected as the defined speed bump did not cause major disturbance to the car. Nevertheless, some body parts show a decrease in vertical acceleration of up to 20% of the original value.

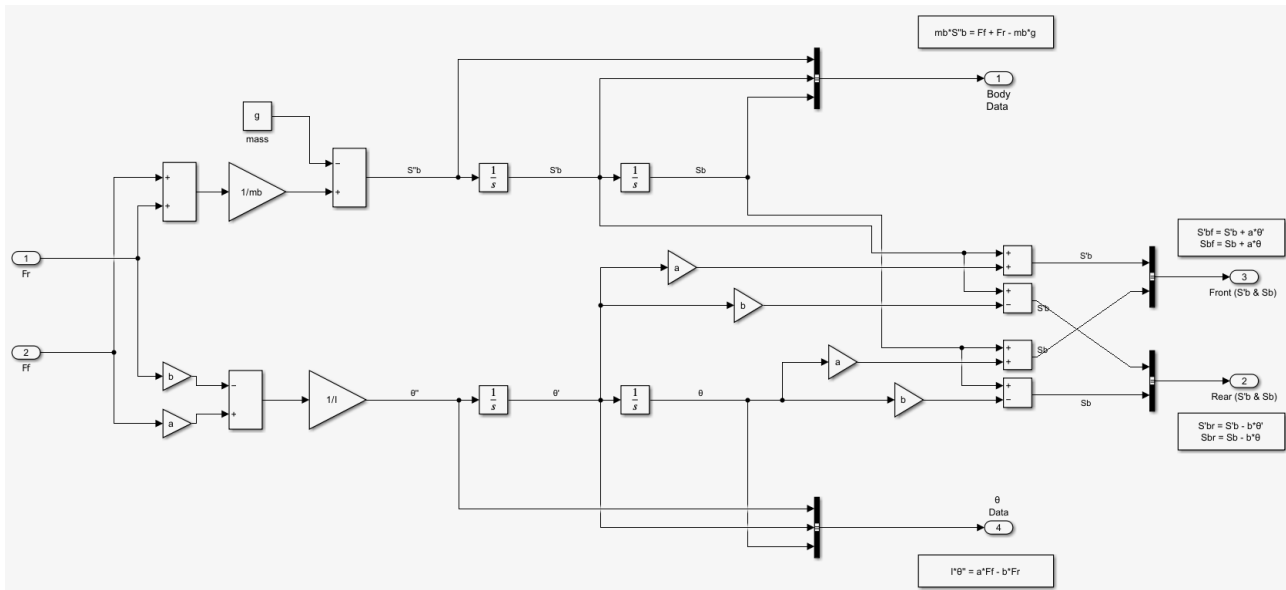
## A APPENDIX: SOURCE CODE

**Listing 1.** Model parameters used in testing and simulations

```

1 %% Code initialisation parameters
2
3 % Wheel parameters
4 Mw = 20;          % Wheel mass (kg)
5 Kt = 14e4;        % Wheel stiffness (N/m)
6
7 % Suspension parameters
8 Ks = 2e4;          % Spring stiffness (N/m)
9 Csc = 600;         % Bumping rate contraction (Ns/m)
10 Cse = 1200;        % Bumping rate extension (Ns/m)
11 Kstiff = 20;       % Spring hardening (*Ks)
12 x0 = 0.2;          % Spring hardening point (m)
13
14 % Body parameters
15 a = 1.35;          % Front wheel distance from CoG (m)
16 b = 1.5;           % Rear wheel distance from CoG (m)
17 Mb = 700;          % Body mass (kg)
18 I = 650;           % Body inertia (kg/m^2)
19
20
21 g = 9.81;          % Gravitational acceleration (m/s^2)
22
23 % Test parameters
24 lambda = 1;         % Sinusoidal road wavelength (m)
25 A = [0.01, 0.05, 0.1]; % Sinusoidal road amplitudes (m)
26 v = [1, 2, 3, 5, 8, 10]; % Vehicle speed (m/s)
27
28 h = 0.1;            % Bump height (m)
29 L = 3.7;             % Bump length (m)
30 d = 3;              % Seminole bump top length (m)

```

**Figure 28.** Simulink body subsystem

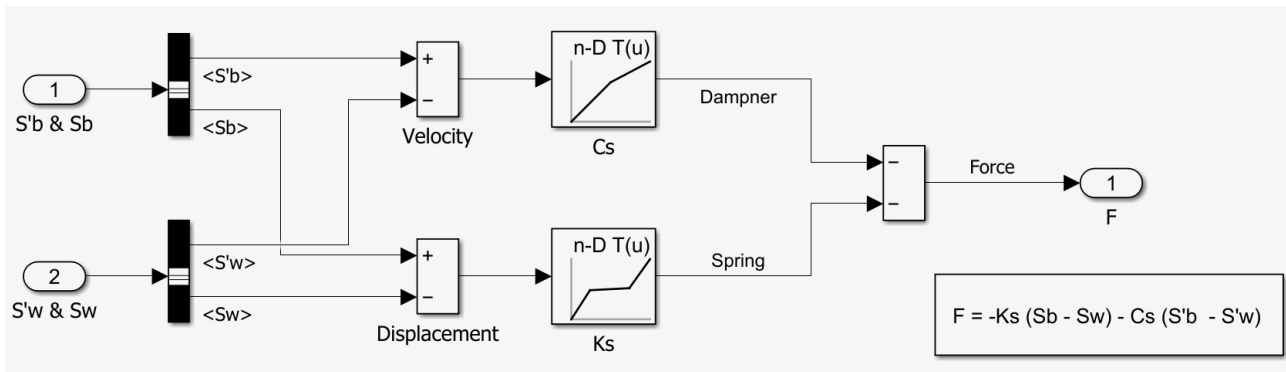


**Figure 29.** Simulink suspension subsystem

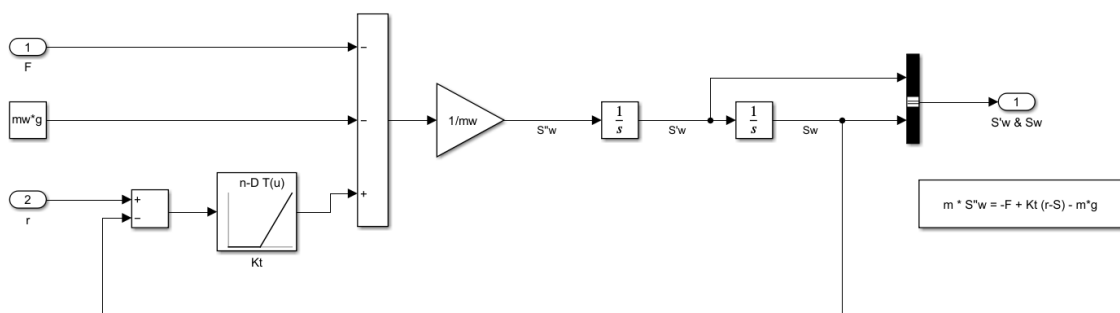


**Figure 30.** Simulink wheel subsystem

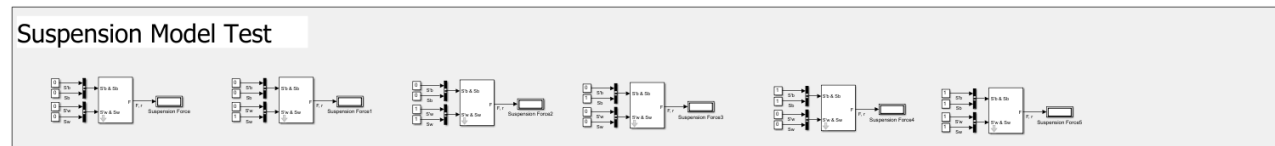
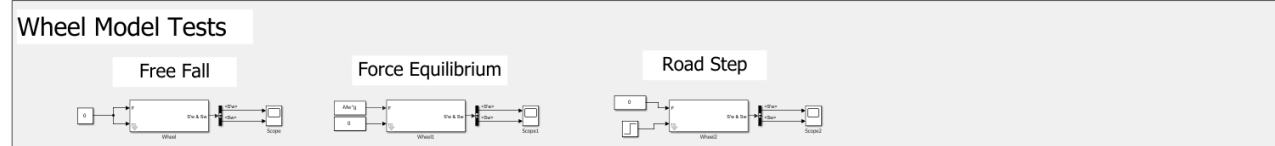
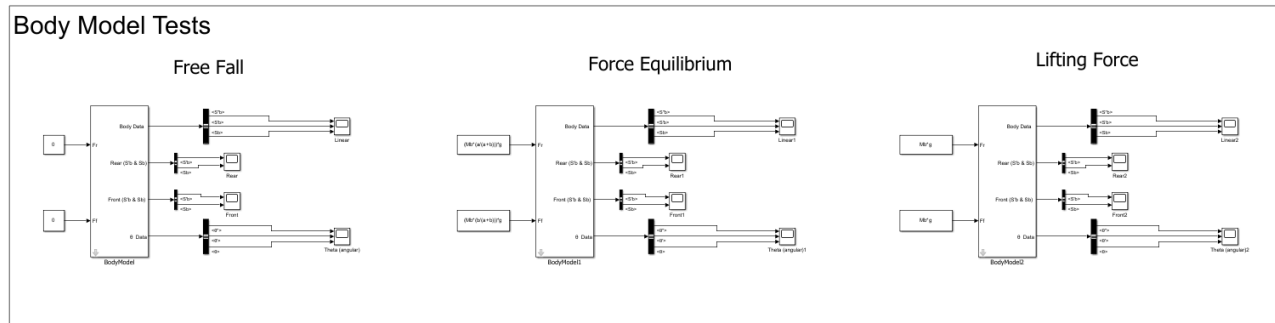


**Figure 31.** Simulink tests for each subsystem of the car model

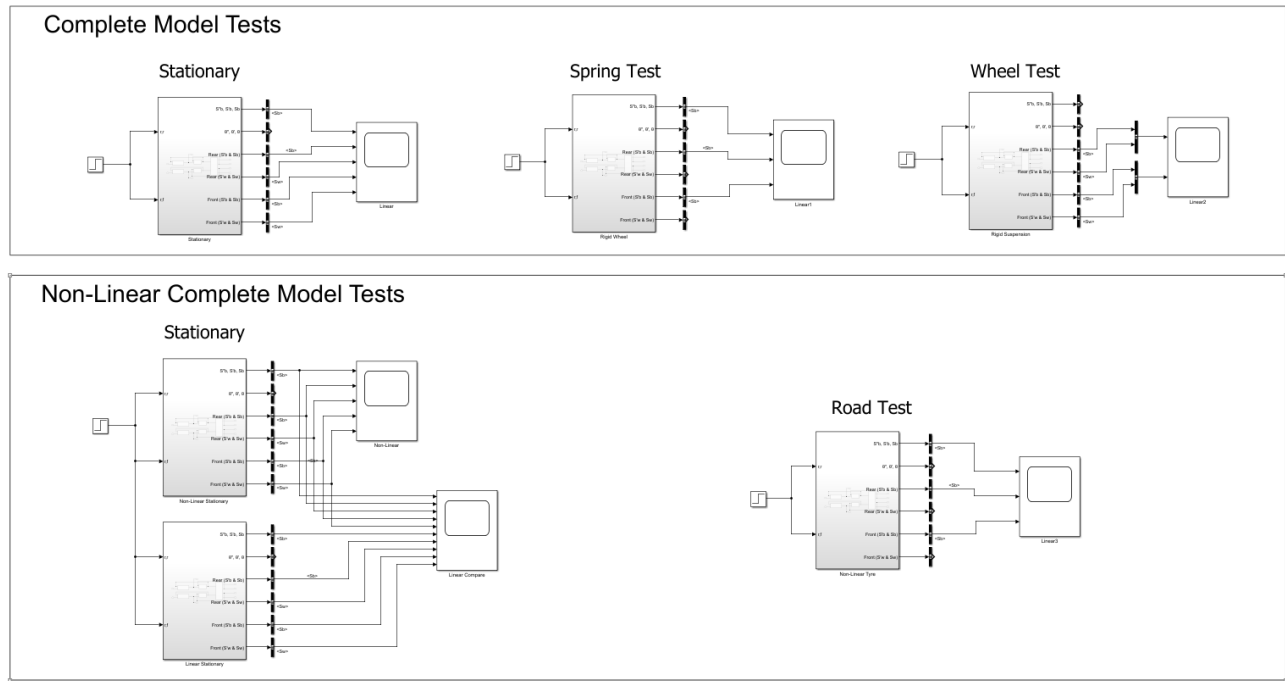


Figure 32. Simulink tests for the car model

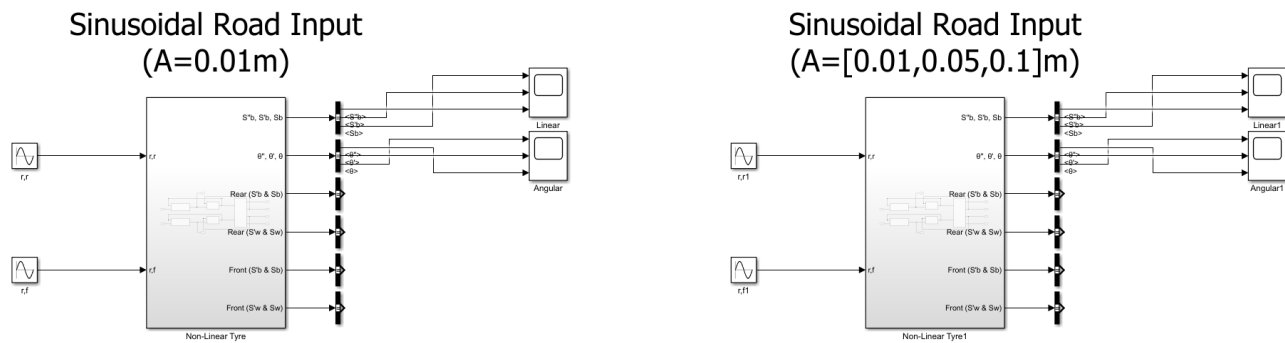


Figure 33. Simulink tests for sinusoidal road effect

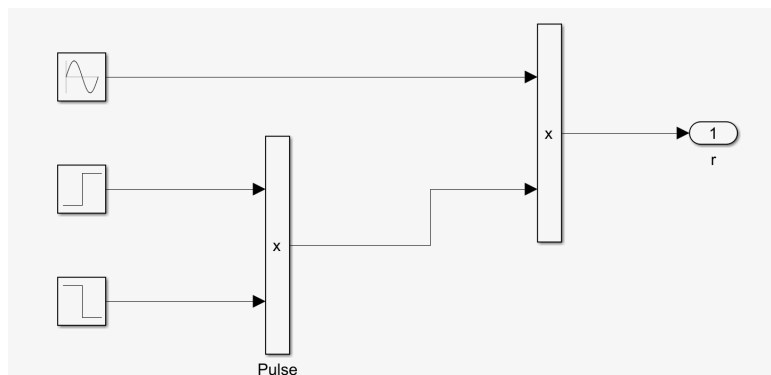
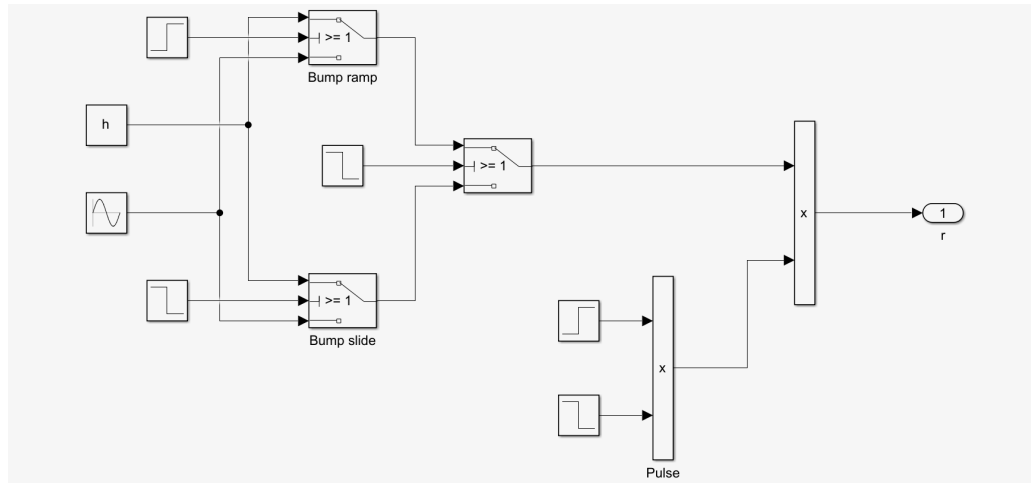
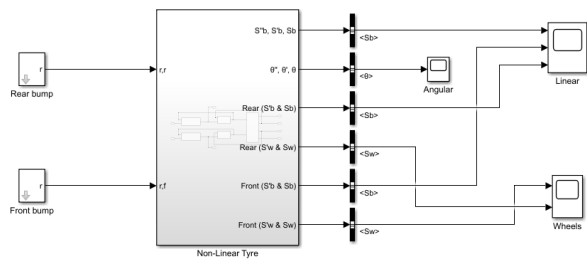


Figure 34. Simulink setup for a Watts profile speed bump



**Figure 35.** Simulink setup for a Seminole profile speed bump

Watts profile



Seminole profile

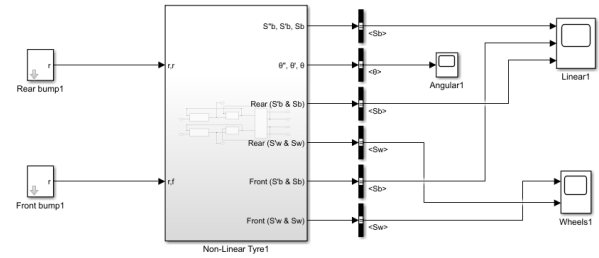


**Figure 36.** Simulink tests for different speed bumps effects

Seminole profile

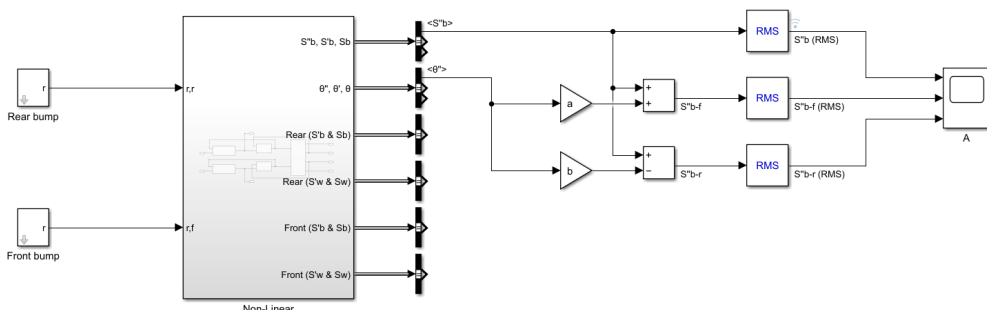


**Figure 37.** RMS calculations for vertical body acceleration at front, rear and centre of mass

## Optimisation comparison

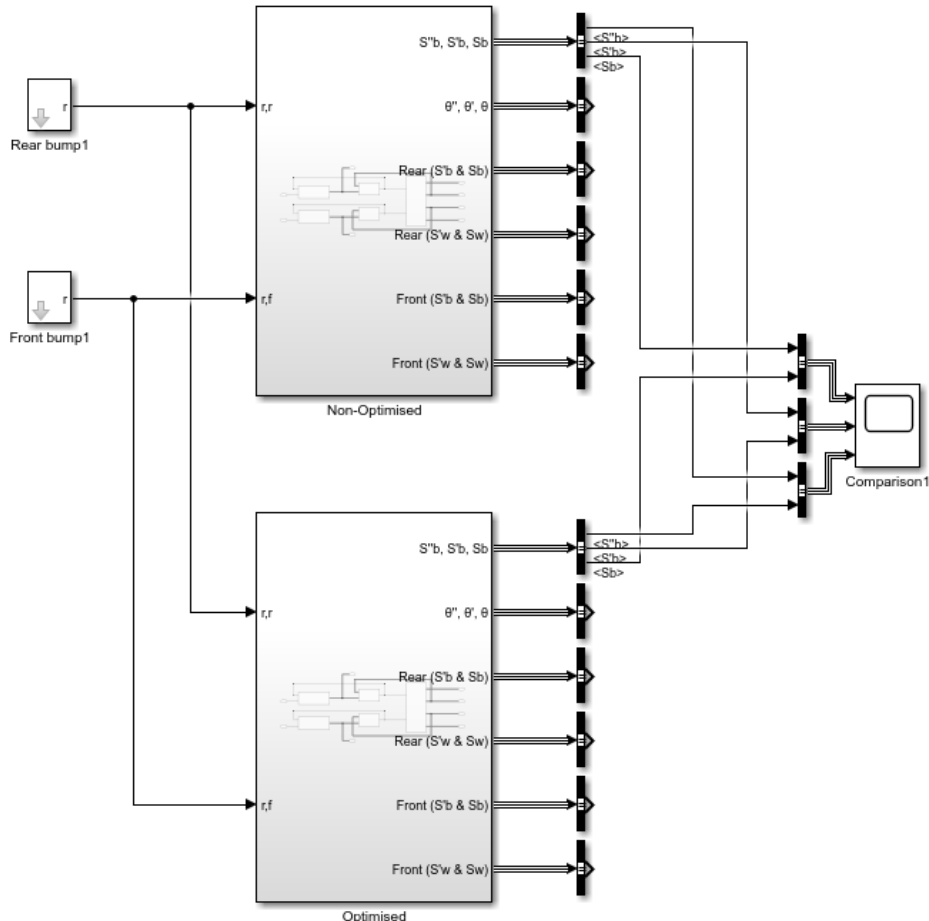


**Figure 38.** Simulink comparison between the non-optimised and the optimised suspension

## REFERENCES

- Antić, B., Pešić, D., Vučić, M. and Lipovac, K., 2013. The influence of speed bumps heights to the decrease of the vehicle speed – belgrade experience. *Safety science* [Online], 57, p.303–312. Available from: <https://doi.org/10.1016/j.ssci.2013.03.008>.
- Brancourt, M., 2017. Ralentisseur de type dos-d'âne et passage piétons - aix-les-bains [Online]. Available from: [https://commons.wikimedia.org/wiki/File:Ralentisseur\\_de\\_type\\_dos-d%C3%A2ne\\_et\\_passage\\_pi%C3%A9tons\\_-\\_Aix-les-Bains.jpg](https://commons.wikimedia.org/wiki/File:Ralentisseur_de_type_dos-d%C3%A2ne_et_passage_pi%C3%A9tons_-_Aix-les-Bains.jpg) [Accessed 2023-12-26].
- Cookson, A., 2023. Assignment 2: *Simulink Modelling of Dynamic Systems*. University of Bath. Unpublished.
- ISO, 2018. ISO 2631-5 mechanical vibration and shock - evaluation of human exposure to whole-body vibration. Geneva: ISO.
- Shwaly, S.A., Zakaria, M.H. and Al-Ayaat, A.H., 2018. Development of ideal hump geometric characteristics for different vehicle types “case study” urban roads in kafr el-sheikh city (egypt). *Advances in civil engineering* [Online], 2018, p.1–12. Available from: <https://doi.org/10.1155/2018/3093594>.